DMD Fast Forward. Published on April 16, 2007 as doi:10.1124/dmd.106.014274

Title page

Abcg2/Bcrp1 mediates the polarized transport of anti-retroviral nucleosides Abacavir and Zidovudine

Guoyu Pan[1], Nagdeep Giri[1], William F. Elmquist.

Department of Pharmaceutics, University of Minnesota, 308 Harvard Street SE

Minneapolis, Minnesota, USA 55455

DMD Fast Forward. Published on April 16, 2007 as DOI: 10.1124/dmd.106.014274
This article has not been copyedited and formatted. The final version may differ from this version.

Running title page

Running title: Bcrp1-mediated transport of Abacavir and Zidovudine (AZT)

Corresponding author:

William F. Elmquist, Ph.D.,

Department of Pharmaceutics, University of Minnesota,

308 Harvard Street SE, Weaver-Densford Hall 9-127,

Minneapolis, Minnesota, USA 55455

phone: 612-625-0097

fax: 612-626-2125

e-mail: elmqu011@umn.edu

Text Pages: 16

Figures: 7

References: 39

Abstract: 249 words

Introduction: 703 words

Discussion: 1766 words

Abbreviations: BCRP, breast cancer resistance protein; DMEM, Dulbecco's Modified Eagle Medium; HPLC, high-performance liquid chromatography; MDCK, Madin-Darby canine kidney; MRP, multidrug resistance-associated protein. ABC, Abacavir, BBB, blood-brain barrier; UV, ultra violet; AIDS, acquired immune deficiency syndrome; PCR, polymerase chain reaction; ANOVA, analysis of variance; DPM, disintegrations per minute; OATP, organic anion transporting polypeptide; CNS, central nervous system; HIV-1, human immune deficiency virus-1.

DMD Fast Forward. Published on April 16, 2007 as DOI: 10.1124/dmd.106.014274
This article has not been copyedited and formatted. The final version may differ from this version.

Abstract

The bioavailability and targeted distribution of abacavir (ABC) and zidovudine (AZT) to viral reservoirs may be influenced by efflux transporters. The purpose of this study was to characterize the interaction of these NRTIs with the Abcg2/Bcrp1 transporter, the murine homolog of human BCRP, using a Bcrp1-transfected MDCKII cell model. Intracellular accumulation of ABC and AZT was significantly reduced by ~90% and ~70%, respectively, in Bcrp1-transfected cells when compared to the wild-type cells. Both ABC and AZT showed significantly increased basolateral-to-apical (B-to-A) and decreased apical-to-basolateral (A-to-B) transport in Bcrp1 cells when compared to wild-type directional flux. The efflux ratio (ratio of B-to-A to A-to-B) in Bcrp1-transfected cells was 22 for ABC and 11 for AZT. GF120918 inhibited this difference in accumulation between the two cell variants with an EC_{50} of 1.32 ± 0.3μM for ABC and 0.31 ± 0.1μM for AZT. Potent and highly cooperative inhibition by Ko143 was observed with an EC_{50} of 121 ± 5nM for ABC and 19.2 ± 1.5nM for AZT (Hill coefficient ~ 3-6). Probenecid, an organic anion inhibitor known to influence AZT biodistribution, had no effect on cellular accumulation in the Bcrp1 model. These studies characterize the Bcrp1-mediated transport of ABC and AZT and show that prototypical BCRP inhibitors GF120918 and Ko143 can inhibit the Bcrp1-mediated transport of these important anti-retroviral compounds. The functional expression of BCRP at critical barriers, such as the intestinal enterocytes, brain capillary endothelium, and target lymphocytes, could influence the bioavailability and targeted delivery of these drugs to sanctuary sites.

DMD Fast Forward. Published on April 16, 2007 as DOI: 10.1124/dmd.106.014274
This article has not been copyedited and formatted. The final version may differ from this version.

Introduction

Antiretroviral therapy (ART), combines three or more anti-HIV-1 compounds and has proven to be effective in reducing viral load and HIV-1 related mortality (Pomerantz and Horn, 2003). Zidovudine (3'-azido-3'-deoxythymidine , AZT), a nucleoside reverse transcriptase inhibitor (NRTI), was the first drug to be approved for the treatment of HIV-1 (Ezzell, 1987). A number of NRTIs, such as emtricitabine (FTC), zalcitabine (ddC), stavudine (d4T), lamivudine (3TC), didanosine (ddI), tenofovir and abacavir (ABC) have since been approved. Standard combination therapy of HIV-1 infection often includes a dual NRTI 'back-bone' with the addition of a protease inhibitor or a non-nucleoside reverse transcriptase inhibitor (Werber, 2003). Both ABC and AZT (Figure 1) are frequent components of combination therapies that have proved to be effective for HIV-1 treatment, for example, indinavir + AZT/d4T + 3TC (Baker, 1997) and (abacavir + 3TC + AZT (Trizivir)) (Kessler, 2005).

HIV-1 has been shown to penetrate the central nervous system (CNS) and replicate in brain macrophages and microglia (Kure et al., 1991; Bagasra et al., 1996). Moreover, the CNS provides a sanctuary for the virus in the body due to insufficient antiretroviral drug delivery through the blood-brain barrier (BBB) (Pialoux et al., 1997). Numerous studies have implicated efflux transport proteins in the BBB in limiting the CNS distribution of some therapeutic agents (Polli et al., 2003; Park and Sinko, 2005). A number of drug efflux transporters have been identified and localized at the BBB, such as P-gp (Cordon-Cardo et al., 1990), MRPs (Mohri et al., 2000), OATPs (Pizzagalli et al., 2002) and BCRP/ABCG2 (Cooray et al., 2002; Hori et al., 2004).

DMD Fast Forward. Published on April 16, 2007 as DOI: 10.1124/dmd.106.014274
This article has not been copyedited and formatted. The final version may differ from this version.

ABCG2/ BCRP is a relatively new member of the ATP-binding cassette transporter superfamily discovered in mitoxantrone-resistant cell lines that do not overexpress P-gp or the MRPs (Doyle et al., 1998). BCRP has been localized in the plasma membrane (Minderman et al., 2002) of cells forming various tissue barriers like the small intestines, colon, bile canaliculi, placental syncytiotrophoblast and the BBB (Jonker et al., 2000; Cooray et al., 2002). The expression of rat Bcrp1 cDNA was found to be approximately 7-fold higher in the brain capillary fraction when compared to the small intestine in rats, suggesting that this efflux protein may play a significant role in limiting brain distribution of its substrates (Hori et al., 2004). The cellular and tissue distribution and efflux transport function of BCRP may be critical in the absorption, distribution, and efficacy of several anti-HIV1 agents, and their passage across the BBB and blood-placental barrier into protected sites.

The CNS exposure of AZT and other NRTIs has been found to be much lower in the brain when compared to the blood concentrations. Active efflux transport out of the CNS is speculated to be a predominant mechanism limiting these NRTIs distribution to the CNS (Sawchuk and Yang, 1999). ABC has also been shown to have lower CNS exposure when compared to plasma or whole blood in rats, guinea pigs, monkeys and humans.(Daluge et al., 1997; McDowell et al., 1999; Thomas et al., 2001). Currently, there are no reports that identify efflux transport proteins that may be involved in the absorption and distribution of ABC. Recent studies have shown that AZT has decreased cytotoxicity and anti-HIV1 activity in $CD4^+$ T-cells that overexpress the wild-type and mutant variants of the efflux transporter BCRP (Wang et al., 2003). These BCRP overexpressing cell lines were also shown to have a reduced accumulation of AZT which was reversed by the BCRP inhibitor, fumitremorgin C (Wang et al., 2003; Wang et al., 2004). However, the involvement of BCRP in the polarized transport of AZT is yet to be reported and there are no reports regarding the interaction of ABC and BCRP or other efflux transporters.

DMD Fast Forward. Published on April 16, 2007 as DOI: 10.1124/dmd.106.014274
This article has not been copyedited and formatted. The final version may differ from this version.

The objective of this study was to characterize the interaction of ABC and AZT with murine Bcrp1, which is homologous to human BCRP. An *in vitro* MDCKII cell model transfected with Abcg2/Bcrp1 was used to assess this interaction with ABC and AZT. If BCRP is shown to be an important transporter of ABC and AZT at critical barriers, then modulation of BCRP-mediated efflux transport of ABC and AZT may lead to efficacious treatment and improved availability to specific sites of action, such as the CNS sanctuary and the target lymphocytes.

DMD Fast Forward. Published on April 16, 2007 as DOI: 10.1124/dmd.106.014274
This article has not been copyedited and formatted. The final version may differ from this version.

Materials and Methods

Materials

[^{14}C]-AZT and [^{3}H]-ABC were obtained from Moravek Biochemicals (Brea, CA). AZT and AZdU were purchased from Sigma-Aldrich, Inc. (Saint Louis, MO). ABC powder was provided by the NIH AIDS Research and Reference Reagent program. GF120918 was kindly provided by Glaxo-Smith-Kline (Research Triangle Park, NC). Ko143 (Allen et al., 2002) was kindly donated by Dr. Alfred H. Schinkel, The Netherlands Cancer Institute (Amsterdam, Netherlands). GF120918 and Ko143 were solubilized in DMSO (Sigma-Aldrich, Inc., Saint Louis, MO) and diluted to desired concentration in assay buffer (NaCl 122mM, $NaHCO_3$ 25 mM, Glucose 10 mM, HEPES 10mM, KCl 3mM, $MgSO_4 \cdot 7H_20$ 1.2 mM, $CaCl_2 \cdot H_20$ 1.4mM, K_2HPO_4 0.4 mM). The final concentration of DMSO in all solutions (including control group) was less than 0.1%. All other reagents or solvents used were either analytical or high-performance liquid chromatography (HPLC) grade.

Cell culture

MDCK-II wild type and Bcrp1-transfected cell lines (Jonker et al., 2000) were kindly provided by Dr. Alfred H. Schinkel, The Netherlands Cancer Institute. Cells used for all our experiments were between passages 5-15. The cells were cultured in DMEM (Mediatech, Inc., Herndon, VA) supplemented with 10% fetal bovine serum (SeraCare Life Sciences, Inc., Oceanside, CA), penicillin (100 U/ml) and streptomycin (100 µg/ml) (Sigma-Aldrich, Inc., Saint Louis, MO). All other cell culture materials were obtained from BD Biosciences (San Jose, CA).

DMD Fast Forward. Published on April 16, 2007 as DOI: 10.1124/dmd.106.014274
This article has not been copyedited and formatted. The final version may differ from this version.

Intracellular accumulation

The wild-type and Bcrp1-transfected cells were seeded at a density of 2 x 10^5 per well and were grown for 2 to 3 days on 12-well plates (TPP® tissue culture plates) to form confluent epithelial monolayers. For the experiment, the growth media was aspirated and the cells in each well were washed twice with 2 ml of assay buffer, followed by preincubation for 30 minutes with 1 ml of assay buffer. The accumulation experiment involved incubation of these cells for 180 minutes at 37°C in an assay buffer (1 ml) containing tracer concentrations of the radiolabeled ABC or AZT. Assay buffer containing radiolabeled drug was aspirated at the end of incubation period and the cells washed three times with 1 ml of ice-cold phosphate buffered saline. The cells were solubilized by adding 1 ml of 1% Triton X-100 (Sigma-Aldrich, Inc., Saint Louis, MO). Total protein concentration in each well was determined by the BCA™ protein assay kit (Pierce Biotechnology, Inc., Rockford, IL) and the corresponding radioactivity was determined by liquid scintillation counting (LS-6500, Beckman Coulter, Inc., Fullerton, CA). Tracer accumulation in the two cell variants was compared and the results were expressed as a percentage of control (total amount of radioactivity (DPM) accumulated per milligram of protein in the wild-type cell).

Directional transport

The wild-type and Bcrp1-transfected cells were seeded at a density of 2 x 10^5 per well and grown for 3 to 4 days on separate Transwell® permeable supports (Corning Inc., Corning, NY) until they formed a confluent polarized monolayer. The upper compartment of the Transwell® is the apical (A) and the lower compartment is the basolateral (B) side. For the transport experiment, growth medium was aspirated and the cells washed twice and pre-incubated with the assay buffer for 30 minutes. The assay buffer was then replaced with buffer containing tracer quantities of radiolabeled ABC or AZT (<100nM) on the donor side.

DMD Fast Forward. Published on April 16, 2007 as DOI: 10.1124/dmd.106.014274
This article has not been copyedited and formatted. The final version may differ from this version.

Fresh drug-free assay buffer was placed on the receiver side. The assay plates were incubated on an orbital shaker (60 RPM) at 37°C for the entire duration of the experiment except while sampling. 200 µl samples were drawn from the receiver side at 0, 30, 60, and 90 minutes and replaced with fresh drug-free assay buffer. Similarly, 200 µl samples were drawn from the donor side at 0 and 180 minutes and replaced with the assay buffer containing radiolabeled nucleotides at the initial donor concentration. The amount of compound transported was calculated using the specific activities of the radiolabeled nucleotides (0.6Ci/mmol for ABC and 53mCi/mmol for AZT) and compared in the wild-type and transfected cells. AZT and ABC directional transport experiments were also conducted in the presence of 50µM of unlabeled AZT or ABC to evaluate the saturability of [^{14}C] AZT and [^{3}H]-ABC transport.

Inhibitory effect of GF120913 and Ko143

Cellular accumulation experiments were conducted in the presence of inhibitors, where assay buffers containing GF120918 (5µM), Ko143 (200 nM) or probenecid (100µM) were used to pre-incubate the cells and for preparing solutions for the assay. The accumulation of ABC was determined at varying concentrations of GF120918 (0.3125, 0.625, 1.25, 2.5, 5.0 and 10µM) and Ko143 (0, 25, 50, 100, 125, 150, 175, 200 and 400nM). The accumulation of AZT was determined at varying concentrations of GF120918 (0, 0.005, 0.01, 0.025, 0.05, 0.1, 0.25, 0.5, 1.0, 5.0 µM) and Ko143 (0, 0.001, 0.01, 0.1, 0.2, 1, 2, 10, 20, 100 and 200 nM). The data were analyzed by a sigmoid E_{max} model (equation 1) using WinNonlin® software Version 5.0.1 (Pharsight Corporation),

$$Effect = E_0 + \frac{Emax * C^{\gamma}}{(C^{\gamma} + EC_{50}{}^{\gamma})} \qquad \textit{Equation 1}$$

DMD Fast Forward. Published on April 16, 2007 as DOI: 10.1124/dmd.106.014274
This article has not been copyedited and formatted. The final version may differ from this version.

where *effect* is the fold increase in accumulation, seen in the presence of inhibitor, over the Bcrp1 control (without inhibitor). E0 is the cell accumulated DPM/mg protein in the Bcrp1 control, normalized to equal unity. Emax is the fold increase over Bcrp1 control at maximal inhibition, C is the concentration of the inhibitor in the incubating media, γ (gamma) is the shape factor (Hill coefficient) in the sigmoid model, and EC_{50} is the concentration of inhibitor at half-maximal inhibition.

Directional transport assay by HPLC

The directional transport assay was also conducted using unlabeled ABC or AZT to confirm the transport of intact nucleoside. The assay was performed as described above using unlabelled ABC and AZT at a concentration of 5µM each. The samples were stored at -20ºC until analysis. For analysis 100µl samples were spiked with 5ng of AZT and AZdU as internal standards for ABC and AZT, respectively. Then 800µl of ethyl acetate was added and the sample vortexed vigorously for 10 minutes. The supernatant was dried under a flow of liquid nitrogen, reconstitued in 100µl of mobile phase and injected onto a HPLC system. The analysis was performed on a Hypersil-BDS column (C-18, 2.1mm x 150mm, 5µM; Keystone Scientific, Inc.) maintained at 45ºC using a Shimadzu column oven (CTO-10Avp). The HPLC system consisted of a Shimadzu pump (LC-10ATvp), flow control valve (FCV-10ALvp), degasser (DGU-20A5), autoinjector (SIL-10ADvp), system controller (SCL-10Avp) and detector (SPD-10Avp). The flow rate of mobile phase (10mM ammonium phosphate buffer (pH 4.6) and methanol (80:20)) was set at 0.2 ml/min and UV absorbance was measured at 266nM.

DMD Fast Forward. Published on April 16, 2007 as DOI: 10.1124/dmd.106.014274
This article has not been copyedited and formatted. The final version may differ from this version.

Permeability calculations and efflux ratio

The effective directional permeabilities (P_{eff}) of the nucleosides were calculated from the permeability equation (equation 2) using slopes (dQ/dt) obtained in the initial linear range from the amount transported vs. time plots (for up to 90 minutes), where A is the area of the Transwell® membrane and Co is the initial donor conentration. The efflux ratio was determined as the ratio of the P_{eff} calculated in the B-to-A direction divided by the P_{eff} in the A-to-B direction.

$$P_{app} = \frac{\left(\frac{dQ}{dt}\right)}{A * C_0} \qquad \textit{Equation 2}$$

Statistical analysis

Statistical analysis was performed using SigmaStat® 3.1 (SYSTAT Software, Inc.). Groups were compared using simple one-way ANOVA, and the Holm-Sidak method was used for the post hoc multiple comparison procedure with a significance level of $p<0.05$.

DMD Fast Forward. Published on April 16, 2007 as DOI: 10.1124/dmd.106.014274
This article has not been copyedited and formatted. The final version may differ from this version.

Results

Intracellular ABC and AZT accumulation

[^{3}H]-ABC accumulation was decreased significantly (~90%; $p<0.001$) in the Bcrp1-transfected cells when compared to the wild-type cells. GF120918 (5μM) and Ko143 (200nM) could significantly increase ABC accumulation in the transfected cells. However, GF120918 significantly increased the observed levels in the Bcrp1-transfected cells, but inhibition did not completely reverse the efflux to reach levels equivalent as those seen in the wild-type cells. Probenecid (200 μM) had no significant effect on ABC accumulation in the Bcrp1-transfected cells and slightly reduced ABC accumulation in wild type cells (Figure 2A). [^{14}C]-AZT accumulation was decreased significantly (~70%; $p<0.001$) in the Bcrp1-transfected cells when compared to the wild type cells. GF120918 (5μM) and Ko143 (200nM) could increase AZT accumulation in the transfected cells to an equivalent level observed in the wild-type cells. Probenecid (200 μM) had no significant effects on AZT accumulation in the Bcrp1-transfected or wild-type cells (Figure 2B).

Effect-Inhibitor Concentration Relationship: GF120918 and Ko143

Varying GF120918 and Ko143 concentrations were used to evaluate inhibitory effect on the Bcrp1-mediated [^{3}H]-ABC and [^{14}C]-AZT accumulation in the Bcrp1-transfected MDCKII cells (Figure 3A-D). Response (inhibitory effect) was measured as the fold increase in accumulation observed in the presence of inhibitor when compared to the Bcrp1 cells without inhibitor (control). GF120918 exhibited a maximal response at 5μM with an Emax, EC50 and gamma of 4.1 ± 0.3 fold, 1.3 ± 0.3μM and 1.7 ± 0.5, respectively for ABC (Figure 3A), and 8 ± 0.5 fold, 0.31 ± 0.1μM and 0.75 ± 0.1, respectively for AZT (Figure 3B). Ko143 exhibited a maximal response at 200nM with an Emax, EC50 and gamma of 7 ± 0.3 fold, 121 ± 5nM

DMD Fast Forward. Published on April 16, 2007 as DOI: 10.1124/dmd.106.014274
This article has not been copyedited and formatted. The final version may differ from this version.

and 6.1 ± 1.4, respectively for ABC (Figure 3C), and 6.7 ± 0.21 fold, 19.2 ± 1.5nM and 2.73 ± 0.7, respectively for AZT (Figure 3D).

BCRP-mediated Directional Flux of ABC and AZT

Both [^{3}H]-ABC and [^{14}C] AZT showed significant differences in directional transport between the wild-type and Bcrp1-transfected cells (Figures 4-7). There was a significantly higher basolateral-to-apical (B-toA) flux and lower apical-to-basolateral (A-to-B) flux of [^{3}H]-ABC in the Bcrp1-transfected cells when compared to the wild type (Figure 4A). GF120918 and Ko143, known Bcrp1 inhibitors, decreased this difference in directional flux of ABC in the Bcrp1-transfected cell lines (Figure 5A and 5C). From these data, the effective directional permeabilities (P_{eff}) of ABC were calculated as described in the methods section. The efflux ratio of Peff in the Bcrp1-transfected cells was calculated to be approximately 22-fold greater than in the wild-type cells (Figure 4B). GF120918 and Ko143 could reverse this difference in directional permeabilities in the two cell variants and Ko143 at 200nM was found to almost entirely inhibit this difference in directional permeability (Figure 5B and 5D). For [^{14}C]-AZT, the B-to-A flux was significantly higher and the A-to-B flux was significantly lower in the Bcrp1-transfected cells when compared to the wild type (Figure 4C). GF120918 and Ko143 significantly decreased this difference in directional flux of AZT in the Bcrp1-transfected cell lines (Figure 6A and 6C). From these data, the P_{eff} of AZT were calculated as described in the methods section. The efflux ratio of P_{eff} in the Bcrp1-transfected cells was calculated to be approximately 11-fold greater than in the wild-type cells (Figure 4D). Both GF120918 and Ko143 could almost entirely reverse this difference in directional permeabilities in the two cell variants (Figure 6B and 6D).

DMD Fast Forward. Published on April 16, 2007 as DOI: 10.1124/dmd.106.014274
This article has not been copyedited and formatted. The final version may differ from this version.

Directional transport of intact nucleosides

Directional transport studies using unlabeled ABC and AZT measured by HPLC confirmed the transport of intact nucleosides in the tracer studies. For both unlabeled ABC and AZT the basolateral-to-apical flux was significantly higher and the apical-to-basolateral flux was lower in the Bcrp1-transfected cells when compared to the wild type (Figure 7A and 7B). When plotted as a percentage of intial donor concentrations over time, there are similar profiles for both radiolabeled and unlabeled ABC and AZT (Figure 7A and 7B) and there was no difference in calculated permeabilities, indicating that for the expeimental time and system, the radiolabel was a good indicator of intact ABC and AZT transport.

DMD Fast Forward. Published on April 16, 2007 as DOI: 10.1124/dmd.106.014274
This article has not been copyedited and formatted. The final version may differ from this version.

Discussion

Numerous studies have reported the CNS distribution of ABC, AZT and other NRTIs to be low and it has been suggested that an active efflux transporter system is partially responsible for limiting CNS distribution of nucleosides (McDowell et al., 1999; Sawchuk and Yang, 1999; Thomas et al., 2001). ABCG2/BCRP is a recently discovered member of the ATP-binding cassette family of transport proteins. This efflux transporter was discovered in mitoxantrone-resistant cell lines that do not over express P-gp or the MRPs (Doyle et al., 1998). BCRP is localized in the plasma membrane of drug resistant tumor cells (Scheffer et al., 2000) and is found in barrier cells of various tissues like the small intestines, colon, bile canaliculi, placental syncytiotrophoblast (Maliepaard et al., 2001) and it has been recently described in the endothelial cells of the cerebral microvasculature (blood-brain barrier) (Cooray et al., 2002). These cellular and tissue expression sites indicate that BCRP may be important in the absorption, distribution and elimination of its substrates. Moreover, recent studies have shown that human BCRP over-expressing cells showed a diminished intracellular accumulation and anti-HIV activity of the NRTIs AZT and 3TC (Wang et al., 2004). The increased resistance of the BCRP over-expressing MT4 lymphocytes strongly suggested that the NRTI, AZT, is a substrate of human BCRP (Wang et al., 2004), leading to ineffective intracellular concentrations of AZT and its active metabolites. Therefore, if AZT and other anti-HIV1 nucleosides prove to be avid substrates for BCRP-mediated transport, this efflux transporter could be important in limiting oral absorption, altering distribution to sites of efficacy and toxicity such as the CD4-positive lymphocytes, and finally, influencing blood-brain barrier penetration which would limit entry into important viral sanctuary sites such as the CNS.

In the current studies, we employed *in vitro* cell monolayers, both parental MDCKII cells and MDCKII cells transfected with Bcrp1 (Jonker et al., 2000), the murine homolog of human BCRP, to evaluate the role of BCRP in the directional transport of ABC and AZT. Using real-time PCR and western blot analysis we observed a significantly higher Bcrp1 gene mRNA and protein expression in transfected cells (data not shown). Importantly, these cells maintained a high expression of Bcrp1 without continuous positive selection via a cytotoxic substrate that could influence the expression of other protective efflux transporters, which could confound the results. The functional activity of this model was further evaluated by examining the cellular accumulation of mitoxantrone, a prototypical Bcrp1 substrate. Mitoxantrone cellular accumulation is greatly diminished in the Bcrp1 transfected cells and accumulation can be completely restored by inhibition of Bcrp1 using Ko143 (data not shown). Therefore, from the gene expression and functional model validation studies, we can conclude that the differences in cellular accumulation or directional transport of compounds in these two variants of MDCKII cells (wild-type and Bcrp1 transfected cells) can be attributed to the efflux transporter Bcrp1.

There was a significant decrease in the accumulation of ABC and AZT (~90 and 70%, respectively) in the Bcrp1-transfected cell line when compared to the parental cells. This decrease in cellular accumulation was effectively reversed in the presence of Bcrp1 inhibitors GF120918 and Ko143 (Figures 2A and 2B). Addition of the potent Bcrp1 inhibitor, Ko143, reversed the Bcrp1-mediated transport for both ABC and AZT to yield equivalent cellular accumulation as seen in the parental MDCKII cells. However, GF120918 was able to completely reverse this difference in accumulation of AZT but not for ABC. Ko143 did not significantly enhance AZT accumulation in the parental cells. Meanwhile, there was slight but significant reduction in ABC accumulation in the parental cells, which may be due to an inhibitory effect of Ko143 on its influx. These data indicate that the difference in cellular accumulation of ABC and AZT in these two

DMD Fast Forward. Published on April 16, 2007 as DOI: 10.1124/dmd.106.014274
This article has not been copyedited and formatted. The final version may differ from this version.

cell types is mediated by Bcrp1 efflux, and strongly indicates that both ABC and AZT are substrates for Bcrp1. These data are the first reported evidence for the interaction of ABC with a specific efflux transporter or an active transporter of any type.

Given the strong evidence that ABC and AZT are Bcrp1 substrates, it was then useful to examine whether or not known inhibitors of NRTI active transport at critical sites can also inhibit Bcrp1. Probenecid-sensitive CNS distribution of AZT was previously reported in the rat (Takasawa et al., 1997), adult rhesus monkey (Cretton et al., 1991) and rabbit (Wong et al., 1993; Wang et al., 1997). The influence of probenecid on efflux transport of other NRTIs, such as ddC, ddI and tenofovir (Takasawa et al., 1997; Gibbs and Thomas, 2002; Mallants et al., 2005) has also been reported. Therefore, we investigated the effect of probenecid on Bcrp1 transport to evaluate if the previously reported probenecid alterations of the CNS distribution of AZT and other NRTIs could be in part mediated through Bcrp1 efflux transport. Our results (Figure 2A and 2B) show that probenecid does not influence the Bcrp1-mediated transport of either ABC or AZT. This finding strongly suggests the previously reported effects of probenecid on the blood brain barrier permeability of AZT involves a transport system other than Bcrp1, such as organic anion transporters in the MRP subfamily or the OAT transport systems in the brain capillary endothelial cells (Sun et al., 2003).

These cellular accumulation studies were followed by directional flux studies for ABC and AZT. Compared with cellular accumulation studies, one of the advantages of the directional flux method is that it provides additional information about whether the compound is transported by a particular active transporter if one knows the localization and orientation of that transporter. The directional transport studies confirmed the role of this efflux protein in the polarized transport of ABC and AZT (Figure 4). The calculated directional

DMD Fast Forward. Published on April 16, 2007 as DOI: 10.1124/dmd.106.014274
This article has not been copyedited and formatted. The final version may differ from this version.

permeabilities, for both ABC and AZT, show that, given the known orientation of Bcrp1 in the transfected MDCKII cells (Mohrmann et al., 2005), there was the expected significant increase in the basolateral-to-apical (B-to-A) transport over the apical-to-basolateral (A-to-B) transport in the Bcrp1 transfected cells, which was significantly higher than in the wild-type cells. This Bcrp1-mediated transport of either nucleoside was not saturated even in the presence of a high concentration (50μM of ABC and AZT) of unlabelled nucleoside (data not shown). These concentrations are approximately twenty-fold higher than normal therapeutic ABC and AZT concentrations in the plasma (Donnerer et al., 2003).

The directional transport of ABC and AZT in the Bcrp1-transfected cells could be modulated using Bcrp1 inhibitors GF120918 and Ko143, and Ko143 was able to almost completely abolish this transport for both ABC and AZT (Figure 5C and 6C). However, GF120918 was able to completely abolish Bcrp1-mediated transport of AZT but not ABC (Figure 5a and 6A). Concentration-dependent effects of these inhibitors on the accumulation of ABC and AZT in the transfected cells show that Ko143 is a more potent inhibitor for both ABC and AZT with an EC_{50} of approximately 121 ± 5nM and 19.2 ± 1.5 nM, respectively, compared to approximately 1.32 ± 0.3μM and 0.31 ± 0.1 μM for GF120918 (Figure 3A-D). Hill coefficients (gamma values) were much larger for Ko143 than GF120918 for both ABC and AZT (6.1 vs 1.7, 2.73 vs 0.75, respectively) , which may imply the existence of cooperative inhibition. The mechanism of such an inhibition is unclear, and it is difficult to speculate based on model-fitted shape factors. However, it may be that Ko143 has a different binding site than GF120918 which is more sensitive to small changes in inhibitor concentration. More interestingly though, may be the possibility that Ko143 can exert its inhibitory effects through another mechanism that is not related to direct binding inhibition, but rather one that includes an intermediary signaling step which then lends itself to a switch–like behavior, triggered by a minimum concentration of Ko143. It is known that there is cooperativity in the inhibition of the p-glycoprotein

mediated daunorubicin transport, and the authors indicate that this could be related to interactions between the homologous halves of the p-glycoprotein molecule (Wang, et al., 2000). It is known that Bcrp1 transports as a homodimer or multimer, and as such could be subject to similar cooperative mechanisms of inhibition. However, it is not known whether other Bcrp1 substrates will give similar results as the two nucleosides under current study. Moreover, GF120918 did not completely inhibit the Bcrp-1 mediated accumulation of ABC. These results may explain the inability of GF120918 to be able to completely inhibit the difference in cellular accumulation and directional transport. Further studies are needed to evaluate the probable differences in mechanism of action, or binding sites, of these two inhibitors. The higher EC50 observed for ABC with both the inhibitors of Bcrp1 suggests that it may have a greater affinity for the efflux transporter compared to AZT.

Major obstacles for the successful treatment of HIV1 infection are the emergence of drug resistant strains and the failure of therapeutic agents, such as the NRTIs, to reach the so called viral sanctuary sites like the CNS (Sawchuk and Yang, 1999). The eventual efficacy of anti-retroviral therapy therefore depends not only on reducing the number of viral particles in the blood, but also on the ability of these anti-HIV agents to reach viral reservoirs. P-glycoprotein (P-gp) and the multidrug-resistance associated proteins (MRPs) subfamily of multi-drug resistance proteins have been widely investigated for their influence on the disposition of a diverse array of therapeutic compounds. There is some suggested involvement of MRP4 and MRP5 and not P-gp in AZT efflux (Jorajuria et al., 2004). Meanwhile, there is no direct evidence for the involvement of an efflux transporter limiting the CNS distribution of ABC. Candidate transporters that may influence absorption, distribution and elimination of both ABC and AZT include some of the traditional organic anion transporters and ABCG2/BCRP.

DMD Fast Forward. Published on April 16, 2007 as DOI: 10.1124/dmd.106.014274
This article has not been copyedited and formatted. The final version may differ from this version.

Our results conclusively show that the directional transport of ABC and AZT is mediated by the efflux transporter Bcrp1. BCRP mediated efflux may influence the oral bioavailability and possibly prevent the delivery of these important components of anti-retroviral therapy to the CNS, amniotic fluid and lymphocytes. These results suggest the need for further investigation to determine the *in vivo* contribution of BCRP in the oral bioavailability and disposition of ABC, AZT and other NRTIs used in therapy. Other components of ART, like the protease inhibitors, such as ritonavir, saquinavir and nelfinavir have been found to be effective inhibitors of this efflux transporter (Gupta et al., 2004). Characterizing the role of BCRP in drug-drug interactions during the co-administration of BCRP substrates and/or inhibitors in combination therapy would be important follow-up studies for both the delivery of these NRTIs to target sites and may result in the altered efficacy or toxicity of NRTIs in AIDS therapy.

Acknowledgements

We thank GlaxoSmithKline for kindly providing us with GF120918 and Dr. Alfred H. Schinkel from Netherlands Cancer Institute for generously providing MDCK-Bcrp1 cells and Ko143.

The following reagent was obtained through the NIH AIDS Research and Reference Reagent Program, Division of AIDS, NIAID, NIH: Abacavir, cat#4680 from DAIDS, NIAID.

References

Allen JD, van Loevezijn A, Lakhai JM, van der Valk M, van Tellingen O, Reid G, Schellens JH, Koomen GJ and Schinkel AH (2002) Potent and specific inhibition of the breast cancer resistance protein multidrug transporter in vitro and in mouse intestine by a novel analogue of fumitremorgin C. *Mol Cancer Ther* **1:**417-425.

Bagasra O, Lavi E, Bobroski L, Khalili K, Pestaner JP, Tawadros R and Pomerantz RJ (1996) Cellular reservoirs of HIV-1 in the central nervous system of infected individuals: identification by the combination of in situ polymerase chain reaction and immunohistochemistry. *Aids* **10:**573-585.

Baker R (1997) 3-drug therapy reduces deaths and new AIDS-related illnesses by 50%. *Beta***:**3-4.

Cooray HC, Blackmore CG, Maskell L and Barrand MA (2002) Localisation of breast cancer resistance protein in microvessel endothelium of human brain. *Neuroreport* **13:**2059-2063.

Cordon-Cardo C, O'Brien JP, Boccia J, Casals D, Bertino JR and Melamed MR (1990) Expression of the multidrug resistance gene product (P-glycoprotein) in human normal and tumor tissues. *J Histochem Cytochem* **38:**1277-1287.

Cretton EM, Schinazi RF, McClure HM, Anderson DC and Sommadossi JP (1991) Pharmacokinetics of 3'-azido-3'-deoxythymidine and its catabolites and interactions with probenecid in rhesus monkeys. *Antimicrob Agents Chemother* **35:**801-807.

Daluge SM, Good SS, Faletto MB, Miller WH, St Clair MH, Boone LR, Tisdale M, Parry NR, Reardon JE, Dornsife RE, Averett DR and Krenitsky TA (1997) 1592U89, a novel carbocyclic nucleoside analog with potent, selective anti-human immunodeficiency virus activity. *Antimicrob Agents Chemother* **41:**1082-1093.

Donnerer J, Kronawetter M, Kapper A, Haas I and Kessler HH (2003) Therapeutic drug monitoring of the HIV/AIDS drugs abacavir, zidovudine, efavirenz, nevirapine, indinavir, lopinavir, and nelfinavir. *Pharmacology* **69:**197-204.

Doyle LA, Yang W, Abruzzo LV, Krogmann T, Gao Y, Rishi AK and Ross DD (1998) A multidrug resistance transporter from human MCF-7 breast cancer cells. *Proc Natl Acad Sci U S A* **95:**15665-15670.

Ezzell C (1987) AZT given the green light for clinical treatment of AIDS. *Nature* **326:**430.

Gibbs JE and Thomas SA (2002) The distribution of the anti-HIV drug, 2'3'-dideoxycytidine (ddC), across the blood-brain and blood-cerebrospinal fluid barriers and the influence of organic anion transport inhibitors. *J Neurochem* **80:**392-404.

Gupta A, Zhang Y, Unadkat JD and Mao Q (2004) HIV protease inhibitors are inhibitors but not substrates of the human breast cancer resistance protein (BCRP/ABCG2). *J Pharmacol Exp Ther* **310:**334-341.

Hori S, Ohtsuki S, Tachikawa M, Kimura N, Kondo T, Watanabe M, Nakashima E and Terasaki T (2004) Functional expression of rat ABCG2 on the luminal side of brain capillaries and its enhancement by astrocyte-derived soluble factor(s). *J Neurochem* **90:**526-536.

Jonker JW, Smit JW, Brinkhuis RF, Maliepaard M, Beijnen JH, Schellens JH and Schinkel AH (2000) Role of breast cancer resistance protein in the bioavailability and fetal penetration of topotecan. *J Natl Cancer Inst* **92:**1651-1656.

Jorajuria S, Dereuddre-Bosquet N, Becher F, Martin S, Porcheray F, Garrigues A, Mabondzo A, Benech H, Grassi J, Orlowski S, Dormont D and Clayette P (2004) ATP binding cassette multidrug transporters limit the anti-HIV activity of zidovudine and indinavir in infected human macrophages. *Antivir Ther* **9:**519-528.

Kessler HA (2005) Triple-nucleoside analog antiretroviral therapy: is there still a role in clinical practice? A review. *MedGenMed* **7:**70.

Kure K, Llena JF, Lyman WD, Soeiro R, Weidenheim KM, Hirano A and Dickson DW (1991) Human immunodeficiency virus-1 infection of the nervous system: an autopsy study of 268 adult, pediatric, and fetal brains. *Hum Pathol* **22:**700-710.

Maliepaard M, Scheffer GL, Faneyte IF, van Gastelen MA, Pijnenborg AC, Schinkel AH, van De Vijver MJ, Scheper RJ and Schellens JH (2001) Subcellular localization and distribution of the breast cancer resistance protein transporter in normal human tissues. *Cancer Res* **61:**3458-3464.

Mallants R, Van Oosterwyck K, Van Vaeck L, Mols R, De Clercq E and Augustijns P (2005) Multidrug resistance-associated protein 2 (MRP2) affects hepatobiliary elimination but not the intestinal disposition of tenofovir disoproxil fumarate and its metabolites. *Xenobiotica* **35:**1055-1066.

McDowell JA, Chittick GE, Ravitch JR, Polk RE, Kerkering TM and Stein DS (1999) Pharmacokinetics of [(14)C]abacavir, a human immunodeficiency virus type 1 (HIV-1) reverse transcriptase inhibitor, administered in a single oral dose to HIV-1-infected adults: a mass balance study. *Antimicrob Agents Chemother* **43:**2855-2861.

Minderman H, Suvannasankha A, O'Loughlin KL, Scheffer GL, Scheper RJ, Robey RW and Baer MR (2002) Flow cytometric analysis of breast cancer resistance protein expression and function. *Cytometry* **48:**59-65.

Mohri M, Nitta H and Yamashita J (2000) Expression of multidrug resistance-associated protein (MRP) in human gliomas. *J Neurooncol* **49:**105-115.

Mohrmann K, van Eijndhoven MA, Schinkel AH and Schellens JH (2005) Absence of N-linked glycosylation does not affect plasma membrane localization of breast cancer resistance protein (BCRP/ABCG2). *Cancer Chemother Pharmacol* **56:**344-350.

Park S and Sinko PJ (2005) P-glycoprotein and mutlidrug resistance-associated proteins limit the brain uptake of saquinavir in mice. *J Pharmacol Exp Ther* **312:**1249-1256.

Pialoux G, Fournier S, Moulignier A, Poveda JD, Clavel F and Dupont B (1997) Central nervous system as a sanctuary for HIV-1 infection despite treatment with zidovudine, lamivudine and indinavir. *Aids* **11:**1302-1303.

Pizzagalli F, Hagenbuch B, Stieger B, Klenk U, Folkers G and Meier PJ (2002) Identification of a novel human organic anion transporting polypeptide as a high affinity thyroxine transporter. *Mol Endocrinol* **16:**2283-2296.

Polli JW, Baughman TM, Humphreys JE, Jordan KH, Mote AL, Salisbury JA, Tippin TK and Serabjit-Singh CJ (2003) P-glycoprotein influences the brain concentrations of cetirizine (Zyrtec), a second-generation non-sedating antihistamine. *J Pharm Sci* **92:**2082-2089.

Pomerantz RJ and Horn DL (2003) Twenty years of therapy for HIV-1 infection. *Nat Med* **9:**867-873.

Sawchuk RJ and Yang Z (1999) Investigation of distribution, transport and uptake of anti-HIV drugs to the central nervous system. *Adv Drug Deliv Rev* **39:**5-31.

Scheffer GL, Maliepaard M, Pijnenborg AC, van Gastelen MA, de Jong MC, Schroeijers AB, van der Kolk DM, Allen JD, Ross DD, van der Valk P, Dalton WS, Schellens JH and Scheper RJ (2000) Breast cancer resistance protein is localized at the plasma membrane in mitoxantrone- and topotecan-resistant cell lines. *Cancer Res* **60:**2589-2593.

Sun H, Dai H, Shaik N and Elmquist WF (2003) Drug efflux transporters in the CNS. *Adv Drug Deliv Rev* **55:**83-105.

Takasawa K, Terasaki T, Suzuki H and Sugiyama Y (1997) In vivo evidence for carrier-mediated efflux transport of 3'-azido-3'-deoxythymidine and 2',3'-dideoxyinosine across the blood-brain barrier via a probenecid-sensitive transport system. *J Pharmacol Exp Ther* **281:**369-375.

Thomas SA, Bye A and Segal MB (2001) Transport characteristics of the anti-human immunodeficiency virus nucleoside analog, abacavir, into brain and cerebrospinal fluid. *J Pharmacol Exp Ther* **298:**947-953.

Wang E., Casciano CN, Clement RP, and Johnson WW (2000) Cooperativity in the inhibition of p-glycoprotein-mediated daunorubicin transport: Evidence for half-of-the-sites reactivity. *Arch Biochem Biophys* **383**(1):91-98.

Wang X, Furukawa T, Nitanda T, Okamoto M, Sugimoto Y, Akiyama S and Baba M (2003) Breast cancer resistance protein (BCRP/ABCG2) induces cellular resistance to HIV-1 nucleoside reverse transcriptase inhibitors. *Mol Pharmacol* **63:**65-72.

Wang X, Nitanda T, Shi M, Okamoto M, Furukawa T, Sugimoto Y, Akiyama S and Baba M (2004) Induction of cellular resistance to nucleoside reverse transcriptase inhibitors by the wild-type breast cancer resistance protein. *Biochem Pharmacol* **68:**1363-1370.

Wang Y, Wei Y and Sawchuk RJ (1997) Zidovudine transport within the rabbit brain during intracerebroventricular administration and the effect of probenecid. *J Pharm Sci* **86:**1484-1490.

Werber Y (2003) HIV drug market. *Nat Rev Drug Discov* **2:**513-514.

Wong SL, Van Belle K and Sawchuk RJ (1993) Distributional transport kinetics of zidovudine between plasma and brain extracellular fluid/cerebrospinal fluid in the rabbit: investigation of the inhibitory effect of probenecid utilizing microdialysis. *J Pharmacol Exp Ther* **264:**899-909.

Footnotes

The project was supported by NIH grant NS42549.

Request for reprints may be addressed to:

William F. Elmquist, Ph.D.,

Department of Pharmaceutics, University of Minnesota,

308 Harvard Street SE, Weaver-Densford Hall 9-127,

Minneapolis, Minnesota, USA 55455

e-mail: elmqu011@umn.edu

[1] (GP) and (NG) contributed equally to this work.

DMD Fast Forward. Published on April 16, 2007 as DOI: 10.1124/dmd.106.014274
This article has not been copyedited and formatted. The final version may differ from this version.

Legends

Figure 1 Structures of BCRP inhibitors (Ko143 and GF120918) and nucleoside substrates (AZT and ABC).

Figure 2 Accumulation in the wild-type and (▬) and Bcrp1-transfected (▭) MDCKII cells and effect of GF120918 (5μM), Ko143 (200nM) and probenecid (prob, 200μM). **(A)** [^{3}H]-ABC accumulation in the Bcrp1-transfected cells. **(B)** [^{14}C]-AZT accumulation in the Bcrp1-transfected cells. Results are expressed as mean ± S.D.; n=3 (***, $p<0.001$, compared with wild-type control group; † $p<0.001$ compared to Bcrp1 control group)

Figure 3 The effect of varying concentrations of GF120918 on [^{3}H]-ABC (A); [^{14}C]-AZT (B) and Ko143 on [^{3}H]-ABC (C); [^{14}C]-AZT (D) accumulation in Bcrp1- transfected cells. The data were analyzed by a sigmoid E_{max} model (equation 1). Results are expressed as mean ± S.D. (n=9; ----, Bcrp1 control)

Figure 4 Directional flux **(A)** [^{3}H]-ABC and **(C)** [^{14}C]-AZT across MDCKII cell monolayers. (wild-type:○, transport from A-to-B compartment; ●, transport from B-to-A compartment. Bcrp1-transfected:□, transport from A-to-B compartment; ■ transport from B-to-A compartment). P_{eff} for **(B)** [^{3}H]-ABC and **(D)** [^{14}C]-AZT (closed bars- from the B-to-A direction, open bars A-to-B direction). The results are expressed as mean ± S.D. (n=9) (*** $p<0.001$.compared to wild-type controls)

DMD Fast Forward. Published on April 16, 2007 as DOI: 10.1124/dmd.106.014274
This article has not been copyedited and formatted. The final version may differ from this version.

Figure 5 Directional flux of [^{3}H]-ABC across Bcrp1-transfected MDCKII cell monolayers with and without inhibitors, GF120918 **(A)** and Ko143 **(C).** Absence of inhibitor: ○, transport from A-to-B compartment; ●, transport from B-to-A compartment. Presence of inhibitor: □, transport from A-to-B compartment; ■ transport from B-to-A compartment. The P_{eff} in the presence of GF120918 (C) and Ko143 (D); P_{eff} in the B-to-A direction is significantly reduced in the presence of inhibitors (closed bars). The P_{eff} from the A-to-B direction is significantly increased in the presence of inhibitors (open bars). The results are expressed as mean ± S.D. (n=9; *** p <0.001.compared to wild-type controls)

Figure 6 Directional flux of [^{14}C]-AZT across Bcrp1-transfected MDCKII cell monolayers with and without inhibitors, GF120918 **(A)** and Ko143 **(C).** Absence of inhibitor: ○, transport from A-to-B compartment; ●, transport from B-to-A compartment. Presence of inhibitor: □, transport from A-to-B compartment; ■ transport from B-to-A compartment. The P_{eff} in the presence of GF120918 **(C)** and Ko143 **(D)**; the P_{eff} in the B-to-A direction is significantly reduced in the presence of inhibitors (closed bars). The P_{eff} from the A-to-B direction is significantly increased in the presence of inhibitors (open bars). The results are expressed as mean ± S.D. (n=9; *** p <0.001.compared to wild-type controls)

Figure 7 Directional flux of ABC **(A)** and AZT **(B)** across MDCKII cell monolayers. Solid lines – radiolabeled compounds measured by liquid scintillation counting; Wild-type: ○, transport from A-to-B compartment; ●, transport from B-to-A compartment. Bcrp1-transfected:□, transport from A-to-B compartment; ■ transport from B-to-A compartment. Dashed lines – unlabeled compounds measured by HPLC; Wild-type: Δ, transport from A-to-B compartment; ▲, transport from B-to-A compartment. Bcrp1-

DMD Fast Forward. Published on April 16, 2007 as DOI: 10.1124/dmd.106.014274
This article has not been copyedited and formatted. The final version may differ from this version.

transfected: ▽, transport from A-to-B compartment ; ▼, transport from B-to-A compartment. The results are expressed as mean ± S.D. (n=3)

DMD Fast Forward. Published on April 16, 2007 as DOI: 10.1124/dmd.106.014274
This article has not been copyedited and formatted. The final version may differ from this version.

Figure 1

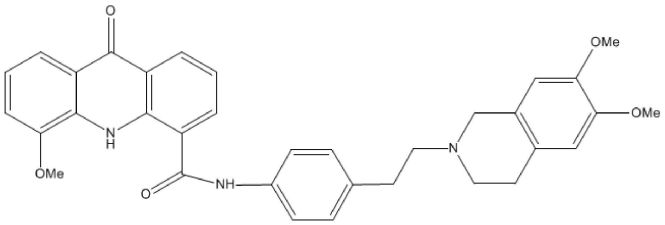

GF120918

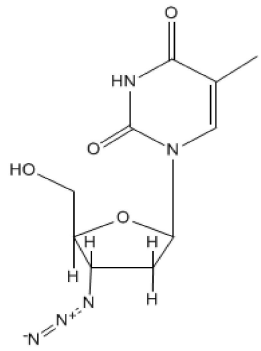

Zidovudine (AZT)

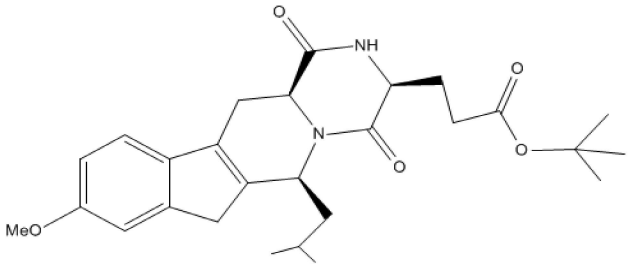

Ko143

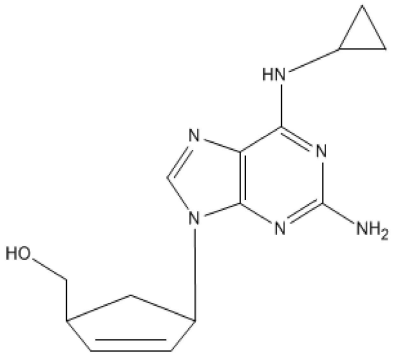

Abacavir (ABC)

DMD Fast Forward. Published on April 16, 2007 as DOI: 10.1124/dmd.106.014274
This article has not been copyedited and formatted. The final version may differ from this version.

Figure 2

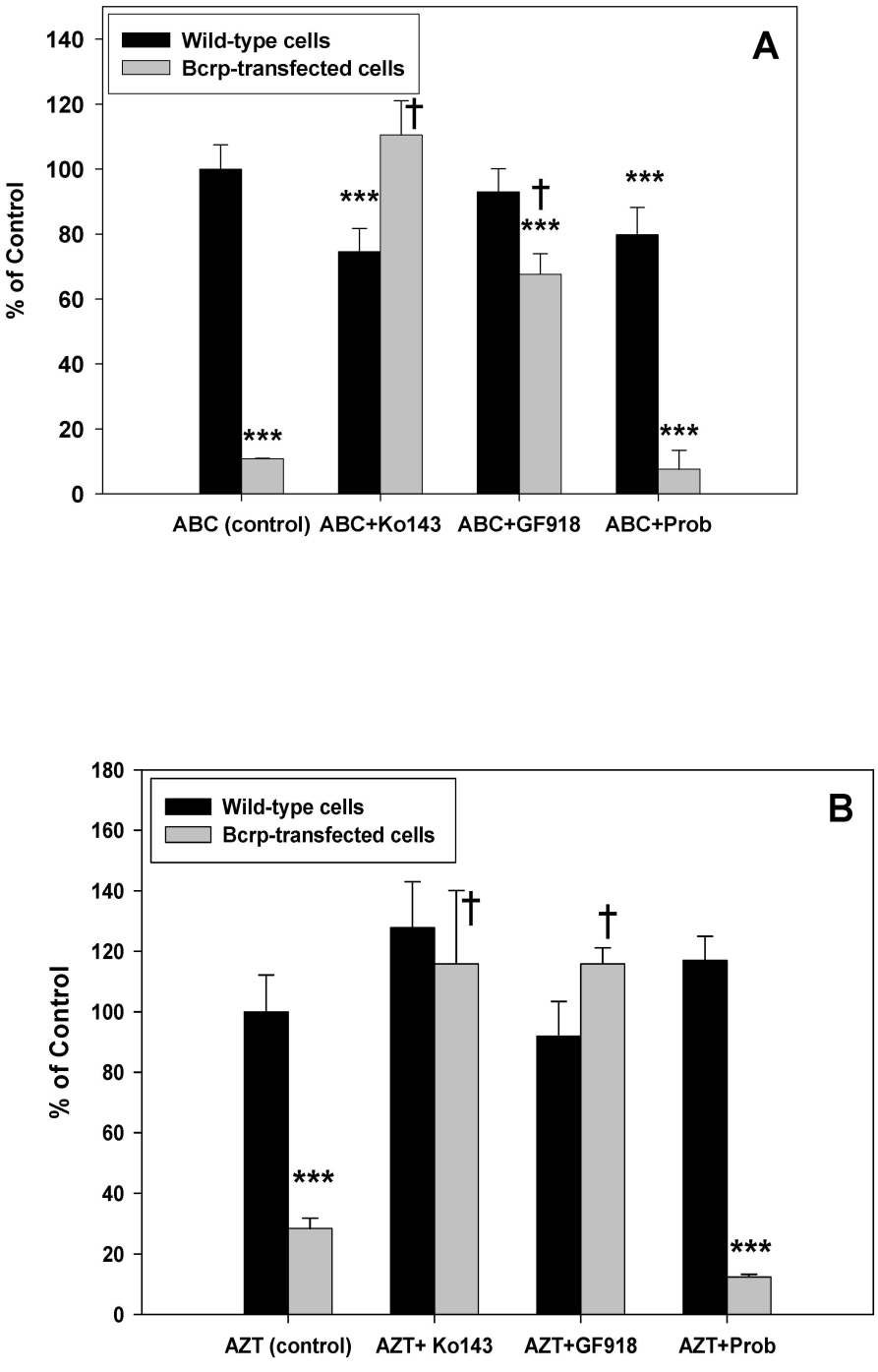

DMD Fast Forward. Published on April 16, 2007 as DOI: 10.1124/dmd.106.014274
This article has not been copyedited and formatted. The final version may differ from this version.

Figure 3

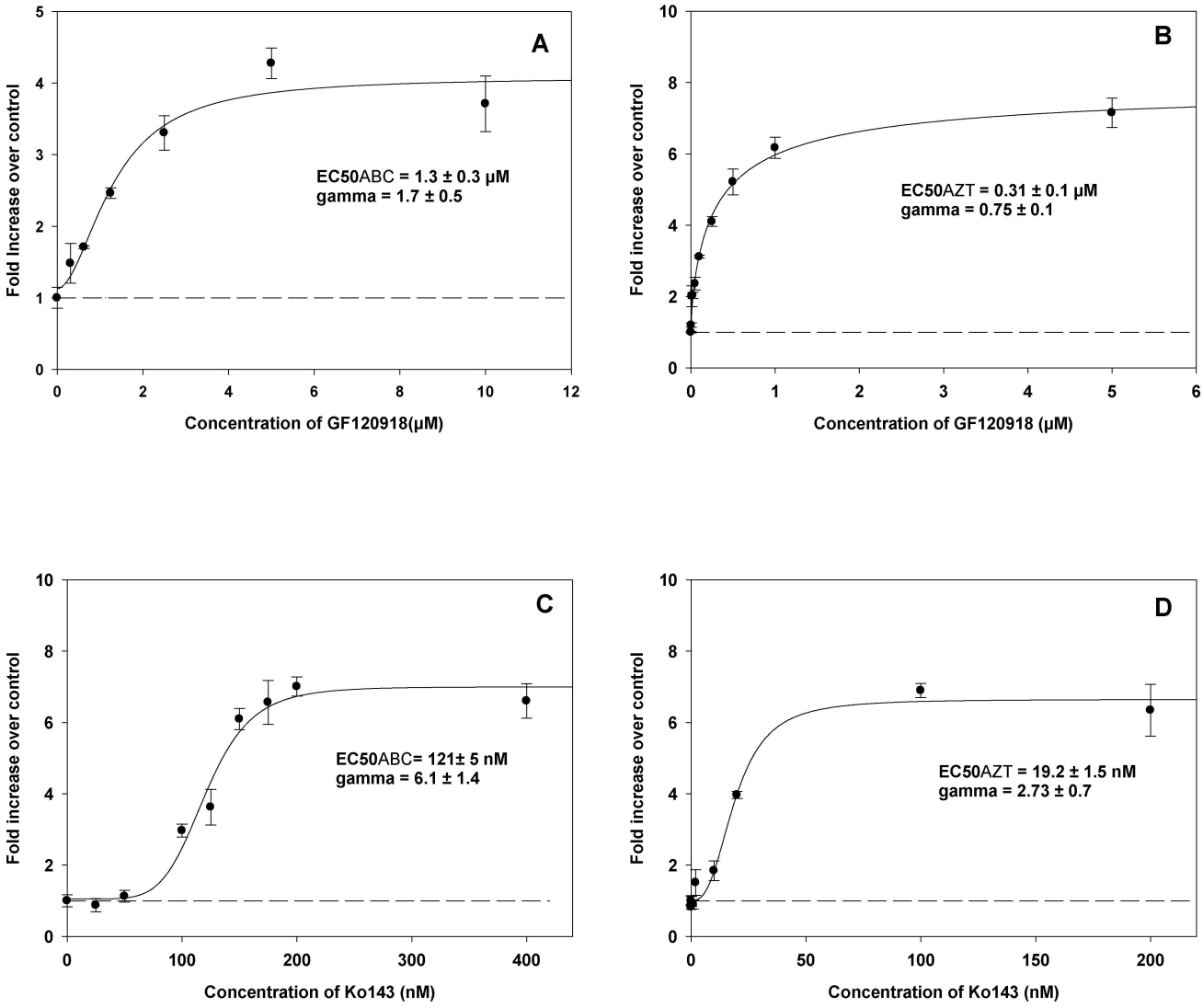

DMD Fast Forward. Published on April 16, 2007 as DOI: 10.1124/dmd.106.014274
This article has not been copyedited and formatted. The final version may differ from this version.

Figure 4

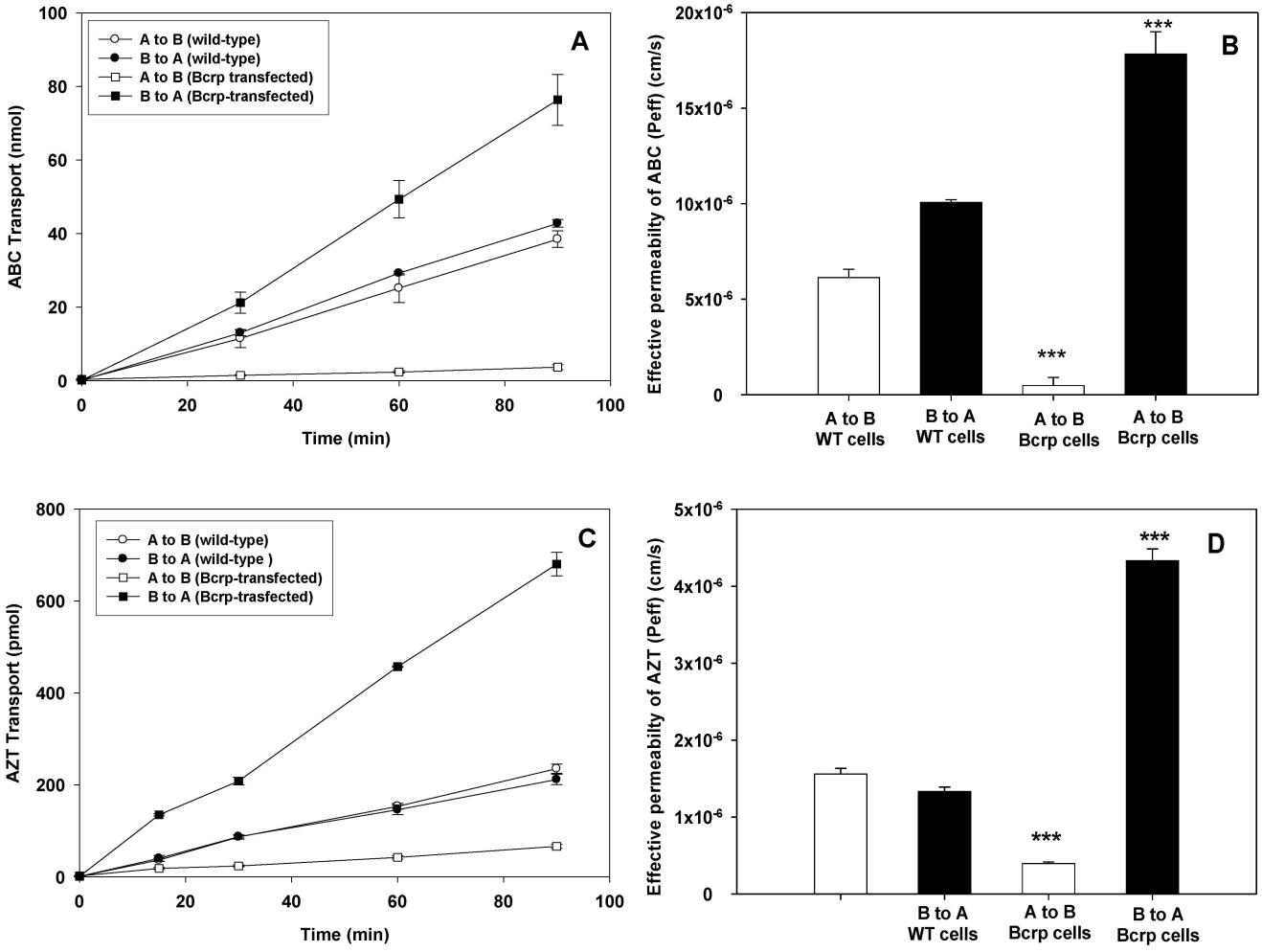

DMD Fast Forward. Published on April 16, 2007 as DOI: 10.1124/dmd.106.014274
This article has not been copyedited and formatted. The final version may differ from this version.

Figure 5

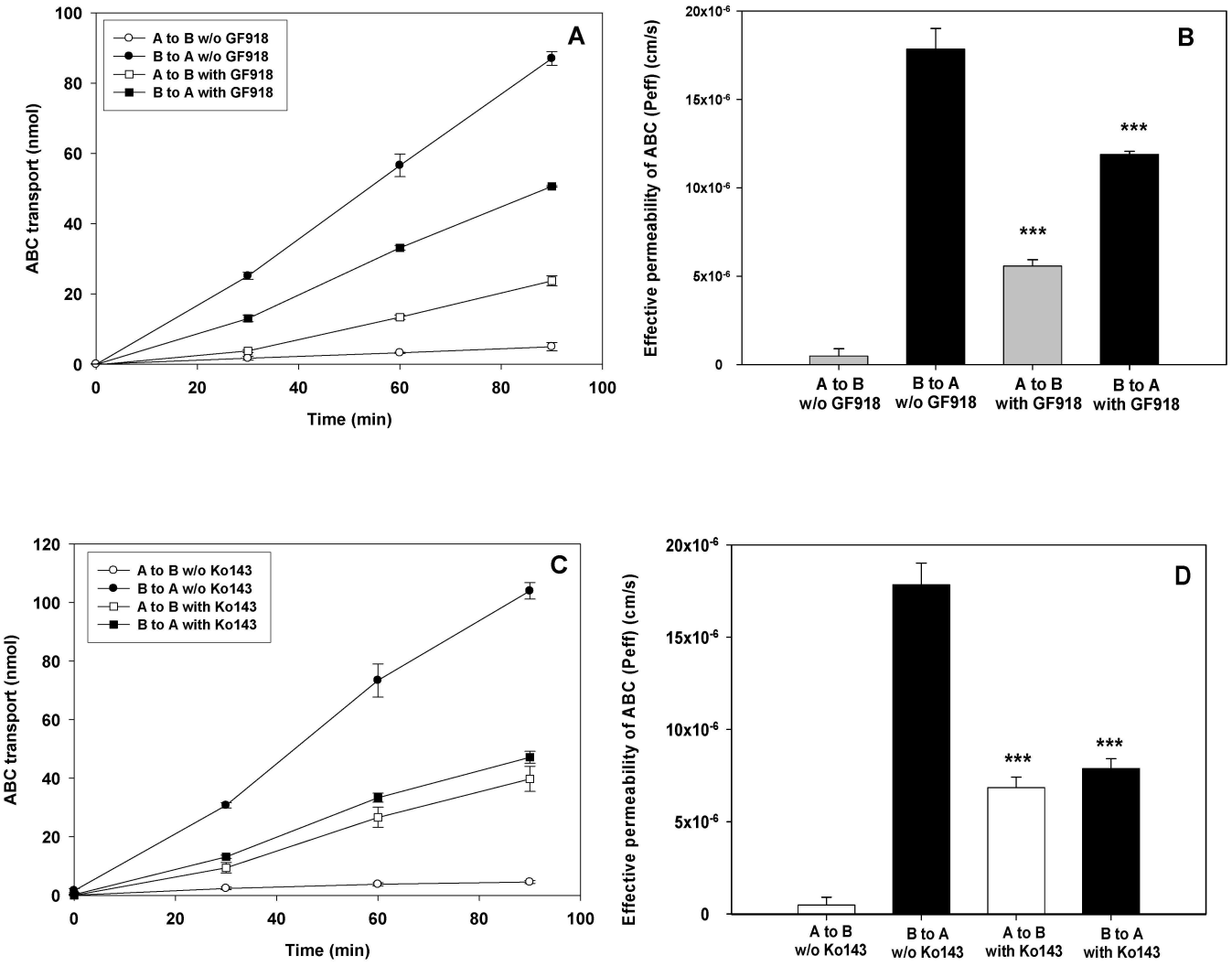

DMD Fast Forward. Published on April 16, 2007 as DOI: 10.1124/dmd.106.014274
This article has not been copyedited and formatted. The final version may differ from this version.

Figure 6

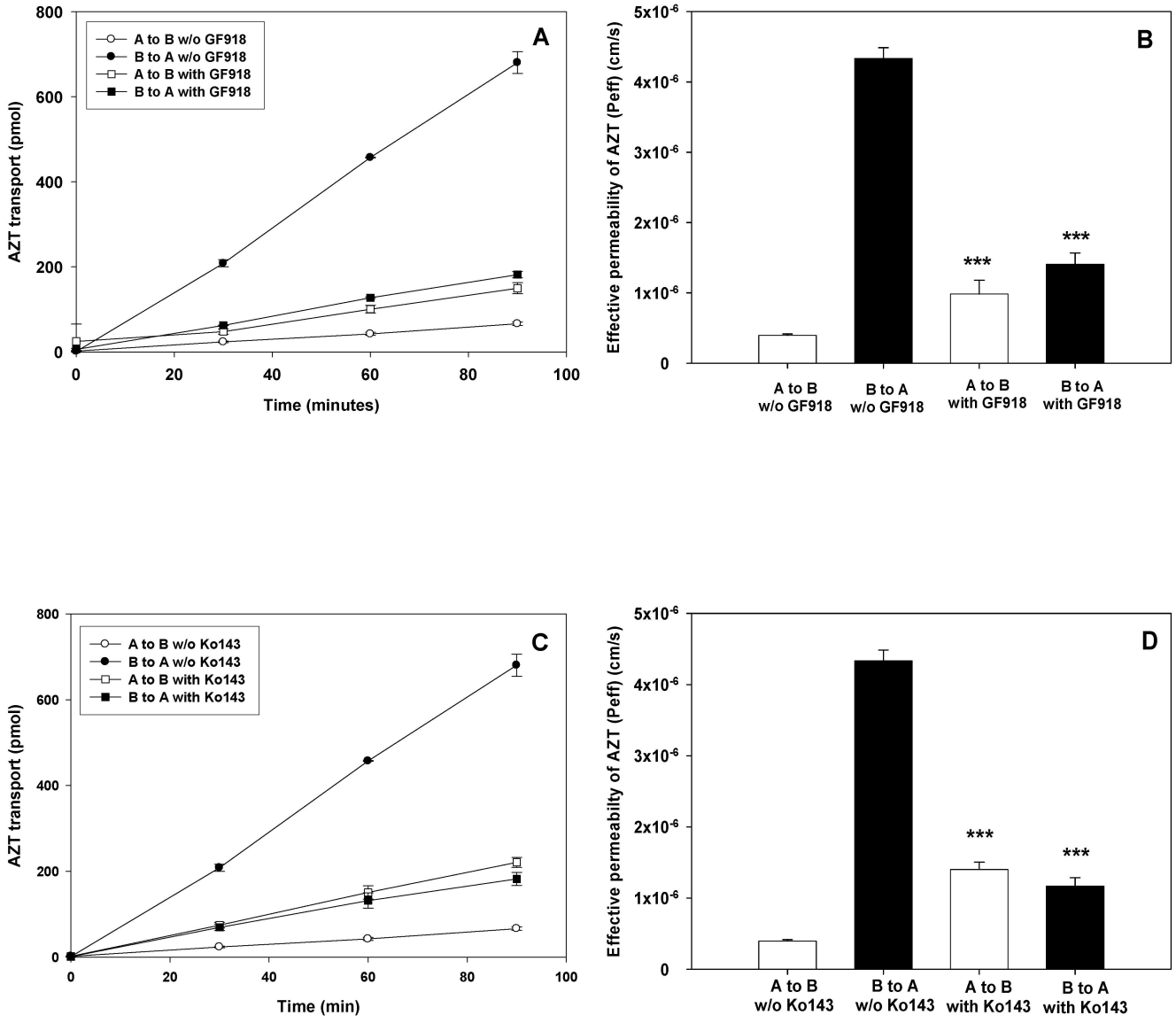

DMD Fast Forward. Published on April 16, 2007 as DOI: 10.1124/dmd.106.014274
This article has not been copyedited and formatted. The final version may differ from this version.

Figure 7